Chinese Journal of
POLYMER SCIENCE

RESEARCH ARTICLE

https://doi.org/10.1007/s10118-026-3632-7
Chinese J. Polym. Sci. **2026**, *44*, 2341–2351

Influence of Antioxidants and Deep Eutectic Solvent on Vulcanization Kinetics and Mechanical Behaviors of Natural Rubber/Styrene-Butadiene Rubber Blend and Composites

Zi-Ye Liu, Yi-Hu Song*, and Qiang Zheng

MOE Key Laboratory of Macromolecular Synthesis and Functionalization, Department of Polymer Science and Engineering, Zhejiang University, Hangzhou 310058, China

Electronic Supplementary Information

Abstract Antioxidants are generally used for prolonging the lifespan of rubber products, while their influences on the vulcanization kinetics and mechanical properties are rarely investigated. Herein, the synergistic roles of conventional antioxidants (6PPD, MB, 2246) and deep eutectic solvent (DES) in natural rubber (NR), styrene-butadiene rubber (SBR), their blends, and the blends filled with carbon black (CB) and black talc (BT) were examined. The results showed that antioxidants and DES influenced the vulcanization kinetics, crosslinking density and mechanical behaviors markedly. A combination of MB and DES resulted in NR/SBR-CB/BT composite vulcanizates with high strength and low dissipation characteristics. DES formed hydrogen bond/ion-pair complexes with antioxidants, and, in NR, interacted with non-rubber constituents, thereby modulating cure intermediates and sulfur-bond distributions, paving the way for preparing high performance rubber composites.

Keywords Natural rubber; Styrene-butadiene rubber; Antioxidant; Deep eutectic solvent; Mullins effect

Citation: Liu, Z. Y.; Song, Y. H.; Zheng, Q. Influence of antioxidants and deep eutectic solvent on vulcanization kinetics and mechanical behaviors of natural rubber/styrene-butadiene rubber blend and composites. *Chinese J. Polym. Sci.* **2026**, *44*, 2341–2351.

INTRODUCTION

Rubber vulcanizates reinforced by fillers[1,2] are widely used in automotive tires, aerospace components, construction damping structures, and everyday products owing to their excellent performance. Vulcanization, which forms a chemically crosslinked network[3], can be regulated by adjusting the accelerator-to-sulfur ratio,[4,5] accelerator system[6,7] and filler[8–10] and by incorporating auxiliary aids to modulate the distribution of sulfur bonds.[11–13] The filler plays a critical role in the reinforcement effect[14] and filler hybridization strategies can improve dispersion[15,16] to optimize the filler network[17] to enhance the mechanical performance.[18]

Rubber blending is common in industries that achieve desired comprehensive performance.[19,20] Natural rubber (NR) exhibits excellent elasticity, fatigue resistance, and mechanical strength, whereas Styrene-butadiene rubber (SBR) exhibits superior wear resistance and wet-skid resistance.[21] Their blends exhibit a unique combination of the advantages of both rubbers.[22] Dynamic covalent networks and sacrificial bonds have been explored to enhance energy dissipation in elastomers,[23–25] but their complex molecular design and uncertain influences on sulfur vulcanization limit their applicability in rubber blends.[26,27] Regulating vulcanization and dissipation through filler design remains a more practical and scalable approach. When fillers are introduced into rubber blends, the compatibility between different rubbers, the filler-rubber interfacial interactions, and vulcanization rates of the rubbers influence the filler dispersion, morphology, and performance.[28,29] Approaches such as the hybridization of different fillers,[30] graft modification of rubber or filler,[31] addition of compatibilizer[32–34] and co-crosslinking of different rubbers[35,36] are used to mediate the performance. However, to date, no studies have addressed the simultaneous regulation of vulcanization kinetics and mechanical behavior of rubber blends.

Under long-term service conditions, rubbers are prone to aging and degradation caused by multiple factors such as heat, oxygen, ozone, and mechanical fatigue.[37,38] The aging leads to chain scission or post-vulcanization, resulting in hardening, cracking, and deterioration of the mechanical properties, severely shortening the lifespan of rubber materials.[39,40] To improve aging resistance, amine- and phenol-type antioxidants are commonly used to scavenge the generated free radicals or decomposed peroxides.[41,42] Great progress by improving anti-aging efficiency,[43] suppressing migration[44] and reducing environmental impact[45] has been achieved[46] while the influence of antioxidants on the net-

* Corresponding author, E-mail: s_yh0411@zju.edu.cn
Received January 4, 2026; Accepted February 24, 2026; Published online May 20, 2026

work architecture and thermo-oxidative resistance remains underexplored.

Recently, deep eutectic solvents (DESs), consisting of hydrogen bond donors and acceptors, have emerged as promising regulators of vulcanization kinetics because of their ability to coordinate with metal oxides and mediate crosslinking reactions.[47] DES acts as a reactive vulcanizing agent to regulate the multiscale structure of NR/SBR blends by improving the ZnO activator dispersion[48] and increasing the crosslinking density (v_c).[47] Herein, the synergistic effects of DES and conventional antioxidants (6PPD, MB, and 2246) on NR, SBR, and their blends were investigated by systematically comparing the vulcanization kinetics, v_c, mechanical performance, and thermo-oxidative aging behaviors. The results revealed that DES accelerates vulcanization and adjusts the crosslinking density depending on the antioxidants. The role of the filler is examined by partially replacing carbon black (CB) with black talc (BT) to balance the reinforcement and aging resistance, where coupling DES with CB/BT hybrid fillers weakens the Mullins softening while maintaining high tensile strength. These findings provide new insights into the use of DES as green additives in rubber composites and offer a feasible strategy for designing efficient anti-aging systems with improved durability.

EXPERIMENTAL

Materials

Natural rubber (NR, SVR3L grade; weight-averaged molecular weight 1120 kg/mol, polydispersity 3.57, and density 0.93 g/cm^3) was purchased from Shanghai Duokang Industrial Co., Ltd. (China). Zinc oxide (ZnO; activator) and *N*,*N*′-diphenylthiourea (DPTU) were obtained from Shanghai Macklin Biochemical Co., Ltd. Styrene-butadiene rubber (SBR, SBR1502, 22.5 wt%–24.5 wt% styrene) was obtained from PetroChina Jilin Petrochemical Co., Ltd. (China). Sulfur and stearic acid (SA; activator) were supplied by Kunshan Anzhe Chemical Stock Co., Ltd. (China) and Tokyo Chemical Industry Co., Ltd. (Japan), respectively. Ethyl acetoacetate, *N*-cyclohexyl-2-benzothiazolesulfenamide (CZ; accelerator), and tetrabutylammonium chloride (TBAC) were supplied by Aladdin Industrial Co., Shanghai (China). Phloroglucinol, *N*-(1,3-dimethylbutyl)-*N*′-phenyl-*p*-phenylenediamine (6PPD; antioxidant), 2-mercaptobenzimidazole (MB; antioxidant) and 2,2′-methylenebis (4-methyl-6-tert-butylphenol) (2246; antioxidant) were purchased from J&K Scientific Co., Ltd. (China), Zhejiang Yongjia Chemical Plant (China), Zhejiang Huangyan Zhedong Rubber Auxiliary Co., Ltd. (China), and Jiangsu Xinluda Polymer Materials Co., Ltd. (China), respectively. Carbon black (CB, N550) with an average particle size of approximately 50 nm and a BET specific surface area of approximately 42 m^2/g was obtained from Cabot Co., Boston, MA (USA). Black talc (BT, 1250 mesh) was supplied by Lingshou Detong Mining Co., Ltd., Hebei (China).

Sample Preparation

DES was synthesized by stirring DPTU and TBAC at a molar ratio of 1:3 in an oil bath at 60.0 °C, yielding a yellow, transparent oily liquid with a melting point of 26.6 °C as determined by differential scanning calorimetry analysis by heating at 5.0 °C/min.

The compounds were formulated to evaluate the effects of the rubber matrix, antioxidant/DES system, and filler composition systematically. Unfilled NR, SBR, and NR/SBR vulcanizates were first prepared to assess the introduction of SBR without compromising the intrinsic performance of NR, with antioxidants added either alone or in combination with the synthesized DES. Based on these systems, filled compounds were further developed by introducing CB or CB/BT fillers to investigate the influence of the hybrid filler networks.

The formulations of the compounds and vulcanizates are provided in Table S1 (in the electronic supplementary information, ESI). Rubber (NR, SBR, or NR/SBR (30/70) blend) was mixed with SA, ZnO, CZ, antioxidants, fillers, and sulfur at 80.0 °C with a rotor speed of 40 revolutions per minute for total 16 min. Antioxidants were added at 2 min of compounding, ZnO and SA at 4 min, DES and fillers at 6 min, and sulfur and CZ at 14 min. Vulcanization was performed using Gotech Testing Machines (GT-7014-E30, Gotech Co., Ltd., Dongguan, China). The vulcanizates were subjected to thermo-oxidative aging in an oven at 100 °C for 48 h to examine their aging resistance.

Characterization

The vulcanizate samples of 1.2–1.5 g were immersed in toluene for 72 h until the swelling equilibrium was reached. The crosslinking density (v_c) was calculated using the Flory-Rehner equation, $v_c = -\frac{\ln(1-V_r)+V_r+\chi V_r^2}{V_s\left(V_r^{1/3}-V_r/2\right)}$.[49] Here V_s=105.7 mL/mol is the molar volume of toluene, V_r is the volume fraction of rubber in the swollen samples, and χ denotes the Flory-Huggins interaction parameter taken as 0.378, 0.391 and 0.346, respectively, for the SBR-toluene, NR-toluene, and NR/SBR (7/3)-toluene pairs, respectively.[50]

Vulcanization curves of the compounds were recorded using a rubber process analyzer (RPA, elite, TA Instruments, USA) at 0.5 Hz and 140 °C. The compounds were sealed in a biconical cavity, 40 mm in diameter, at a clamping pressure of 4.5 MPa.

Attenuated total reflection Fourier-transform infrared (FTIR) spectra were recorded using a spectrometer (Nicolet iS10, Thermo Fisher Sci. Inc., USA) at a resolution of 4 cm^{-1} and scan-coaddition number of 32.

X-ray photoelectron spectroscopy (XPS) was performed using a spectrometer (*X*-Ray005, Thermo Scientific K-Alpha, USA) with an aluminum K alpha with a spot size of 900 μm. The spectra captured by fine scanning (0.1 eV) were calibrated by subtracting the Shirley background and further correcting the C 1s binding energy using a standard value 284.8 eV for hydrocarbon.

The filled vulcanizates frozen in liquid nitrogen were cryomicrotomed into ultrathin sections approximately 100 nm in thickness. The sections were observed using transmission electron microscopy (TEM, JEM-1230, JEOL, Japan) at an accelerating voltage of 120 kV to evaluate the dispersion and distribution of the fillers.

The vulcanizate sheets were cut into dumbbell-shaped specimens of gauge length 25 mm, width 4 mm, and thickness 2 mm. Uniaxial tensile tests were performed using a SANS universal testing machine (UTM2103, Suns Zhongheng Technol. Co., Ltd., Shenzhen, China) at a crosshead speed of 500 mm/min. Cyclic tensile tests were performed at 50

mm/min with a pre-strain of 100%.

RESULTS AND DISCUSSION

Vulcanization Kinetics and Crosslinking Density

Fig. 1 shows the storage modulus (G') as a function of vulcanization time for the compounds at 140 °C. The vulcanization rate of SBR (Fig. 1b) is generally faster than that of NR (Fig. 1a), except for compounds containing the antioxidant 2246. For SBR, the antioxidant 2246 markedly delays the vulcanization whereas MB promotes the vulcanization more rapidly than 6PPD. For NR, these differences are less pronounced. MB containing a moiety similar to the active one of the accelerator CZ (benzothiazole moiety) may form Zn-MB intermediates that facilitate vulcanization. In contrast, the hindered phenolic antioxidant 2246 delays the vulcanization because the steric hindrance interferes with molecular collisions. 6PPD, with a moderate steric hindrance but lacking benzothiazole-based promoting moieties analogous to those in accelerator CZ, behaves as an intermediate vulcanization promotor. For the NR/SBR blends, 2246 is superior to 6PPD and MB in promoting the vulcanization (Fig. 1c). The presence of 50 phr CB (volume fraction φ=0.196; Fig. 1d) or 40 phr CB/10 phr BT (total volume fraction φ=0.193; Fig. 1e) accelerates the vulcanization and reduces the differences in vulcanization kinetics induced by antioxidants.

DES significantly improves the vulcanization rates by shortening induction period and eliminating the differences induced by antioxidants. DES could improve G' in the stage of vulcanization equilibrium (G'_{eq}), except for SBR gum (Fig. 1b). This might be related to the interaction between DES and NR containing 2 wt%–3 wt% non-rubber components[51] mainly composed by proteins and phospholipids. Upon introducing DES, the strong hydrogen-bond donor/acceptor capacity and ionic-pair characteristics of DES enable, on the one hand, associations with proteins and phospholipids and, on the other hand, transient complexation with Zn^{2+}–accelerator fragments, which promote the uniform formation of active intermediates.

In general, G'_{eq} increases with increasing v_c[52,53] (Fig. 1f) while it is slightly affected by antioxidants. Approximately, G'_{eq} of the gum vulcanizates could be described by the modified Gaussian chain network model,[27] $G'_{eq} = (v_c + v_e)RT$. Here v_e=90 mol/m^3 is entanglement density (corresponding to 0.32 MPa being close to plateau modulus (0.38±0.04 MPa for NR[54] and smaller than that of about 0.64 MPa for SBR[55]). For the composites vulcanizates with φ≈0.19, G'_{eq} is approximated by $(v_c+v_e)RT(1-\varphi)A_f^2$ with a strain amplification factor A_f estimated as 1.5. The marked positive deviation of the measured from the predicted G'_{eq} values in the NR/SBR-CB vulcanizates may arise from the synergistic effect between CB and antioxidants, which influences the network structure and reinforces the network additionally.[56]

In general, blending and filling improve v_c while antioxidants and DES strongly influence v_c of the virgin vulcanizates and its relative change after thermo-oxidative aging (Fig. 2). The filling effect is accompanied by chain adsorption on the surface of the filler particles.[57] In the NR, SBR, and NR/SBR gum vulcanizates free of DES, the incorporation of 6PPD yields similar v_c (136–147 mol/m^3). Compared with 6PPD, MB facilitates the formation of highly crosslinked NR vulcanizates, sporadically crosslinked SBR vulcanizates, and similarly crosslinked NR/SBR vulcanizates. On the other hand, 2246 tends to lower v_c in the NR and SBR vulcanizates and improves v_c in the NR/SBR vulcanizates. The effect of DES depends on the antioxidants used. In the absence of antioxi-

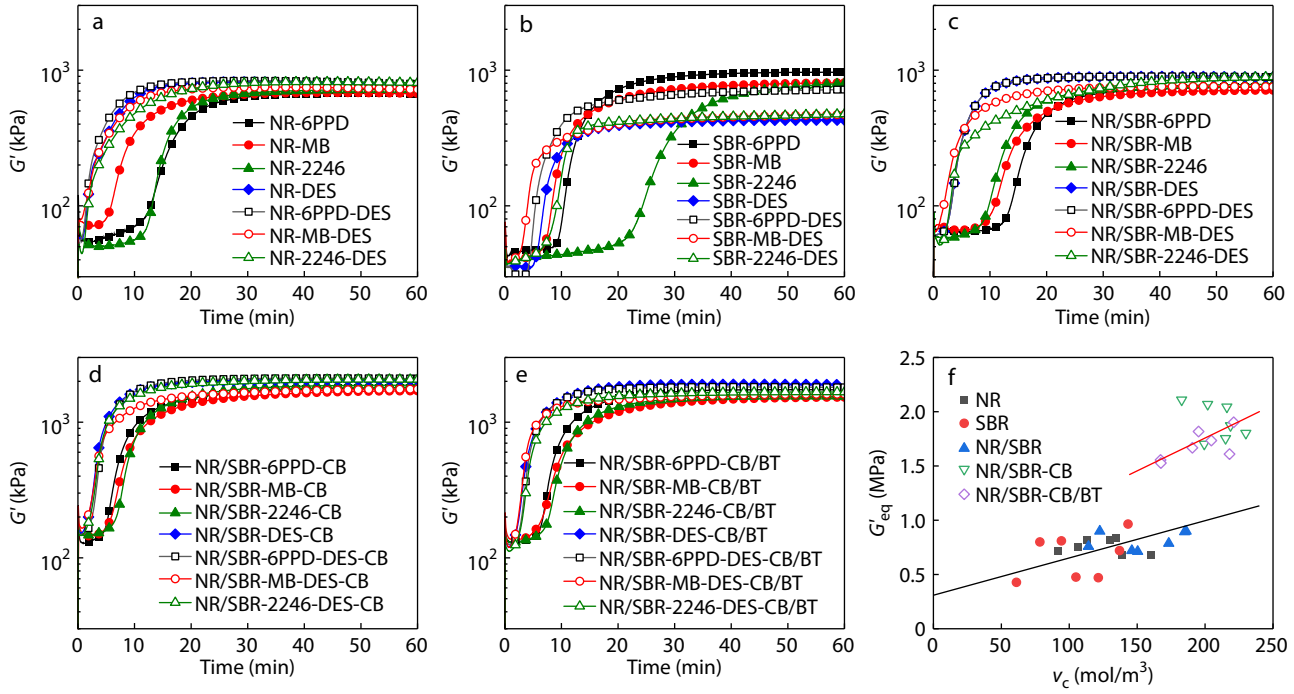

Fig. 1 G' at 140 °C as a function of vulcanization time for NR (a), SBR (b), NR/SBR (c), NR/SBR-CB (d), and NR/SBR-CB/BT compounds (e), and G'_{eq} as a function of v_c for the gum and composites vulcanizates (f). In (f), the solid curves are drawn according to $(v_c+v_e)RT$ for the gums and $(v_c+v_e)RT(1-\varphi)A_f^2$ for the composites vulcanizates, v_e and A_f being estimated as 90 mol/m^3 and 1.5, respectively.

https://doi.org/10.1007/s10118-026-3632-7

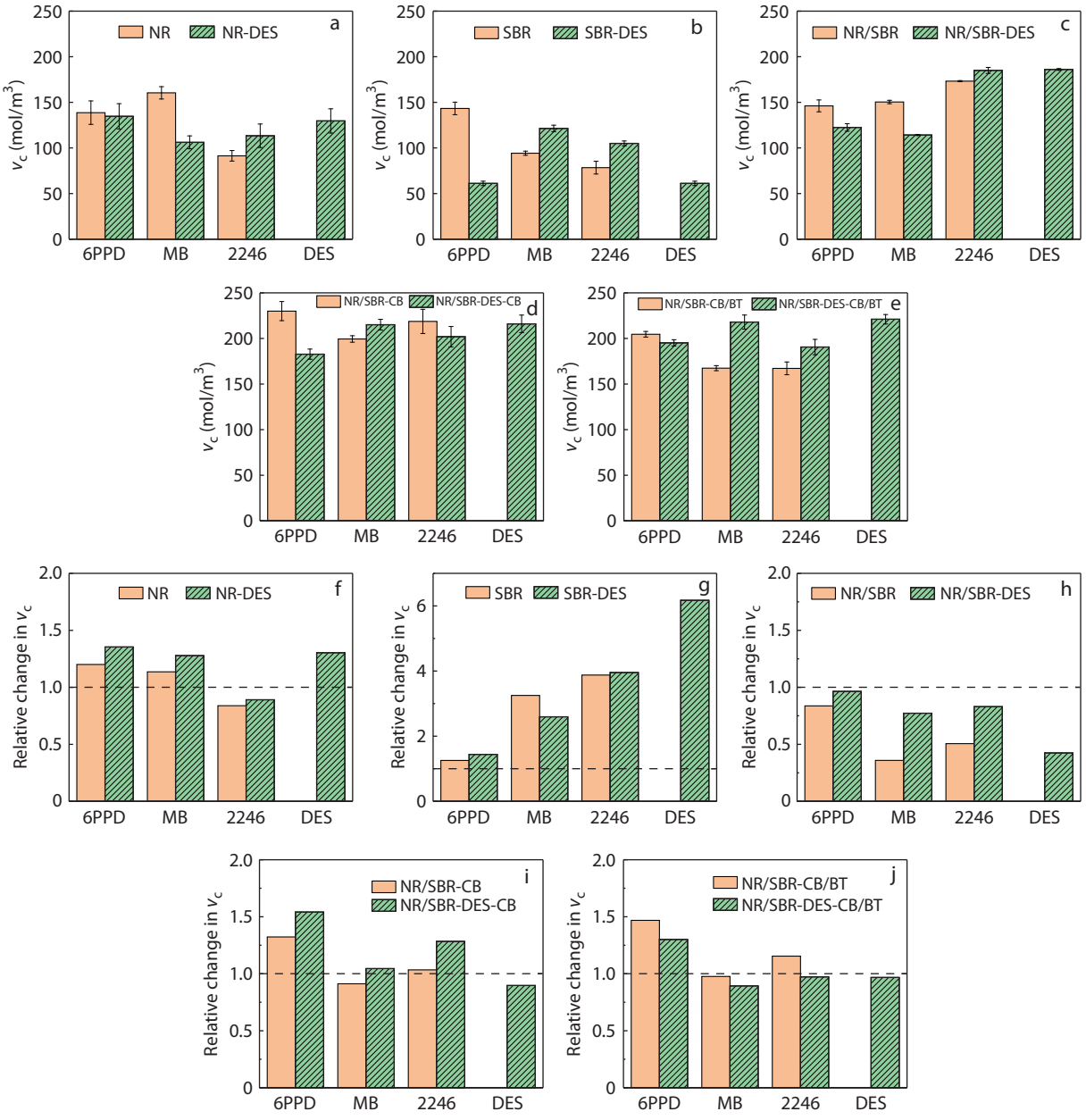

Fig. 2 Influence of DES on v_c (a–e) and its relative change induced by aging (f–j) of the NR (a and f), SBR (b and g), NR/SBR (c and h), NR/SBR–CB (d and i), and NR/SBR–CB/BT vulcanizates (e and j) with different antioxidants.

dants, DES facilitates the formation of a highly crosslinked network in the NR and NR/SBR vulcanizates, while it leads SBR to form a very slightly crosslinked network (v_c=61 mol/m^3), the former being ascribed to the interaction of DES with the non-rubber components in NR. In comparison with 6PPD, co-use of DES and 6PPD lowers v_c in NR, SBR, and NR/SBR vulcanizates. The reverse is true for the co-use of 2246 and DES. In the NR/SBR composites, the combination of DES and antioxidants cause discernible changes in v_c while these changes are substantially attenuated in comparison with the gum stocks.

Except for the NR vulcanizate containing 2246 and DES, aging normally improves v_c of the NR and SBR vulcanizates (Fig. 2), indicating that secondary crosslinking dominates over chain scission during thermo-oxidation. The aging-induced v_c variation of NR is considerably smaller than that of SBR, which could be ascribed to the evolution of the natural associating network constructed by the non-rubber components in NR.[58] In contrast, in the NR/SBR blend vulcanizates, v_c decreases very slightly after aging, suggesting that chain scission occurs, possibly at the interface between the NR and SBR domains, more readily than secondary crosslinking. The introduction of DES lowers the extent of v_c decrement, suggesting that DES participates in network reorganization during thermo-oxidative aging. For the composites, the aging-induced relative v_c changes are in the narrow range of 0.9–1.5, being comparable with those in the NR vulcanizates. Compared with the NR/SBR-CB and NR/SBR-CB/BT composites containing 6PPD, those with MB and DES demonstrate similar v_c and

lowered v_c changes.

Molecular Interactions

The effects of DES and antioxidants on vulcanization are investigated using FTIR and XPS. Fig. 3(a) shows the FTIR spectra of TBAC, DPTU, and DES. A characteristic N—H stretching vibration appears at 3205 cm^{-1} for DPTU while it shifts to 3434 cm^{-1} with marked broadening in DES. The singlet at 921 cm^{-1} and doublet at 892 cm^{-1} belonging to TBAC combine into a strong band at 883 cm^{-1}. Simultaneously, the band at 933 cm^{-1} belonging to DPTU and that at 992 cm^{-1} arising from TBAC disappear in DES. Furthermore, the N—H···Cl^- hydrogen bonding interaction in DES induces a new singlet at 1250 cm^{-1} and multiplate around 1670 cm^{-1} being attributable to imine-like resonance.[59] In the NR and SBR vulcanizates containing 6PPD, DES does not influence the FTIR spectra (Figs. 3b and 3c). In NR containing MB and 2246, DES weakens the bands at 1639 cm^{-1} (amide I of proteins)[60,61] and 1015 cm^{-1} (C—O/C—N stretching and coordination-related modes), suggesting that DES interferes with the vulcanization *via* the H-bond/ion-pair (O—H···Cl^- and N—H···Cl^-) interactions of Cl^- ion in DES with O—H in hindered phenol 2246 or N—H/S—H in MB. In SBR containing MB and 2246, DES introduces new bands at 1408 and 886 cm^{-1} without interfering with the butadiene fingerprints at 966 and 910 cm^{-1},[62] indicating that DES predominantly interacts with arylamine/hindered-phenol antioxidants to improve the vulcanization activity. In the NR/SBR vulcanizates (Fig. 3d), DES weakens the bands at about 1540 cm^{-1} (amide II band of proteins[60,61] and antisymmetric and symmetric stretching of COO— of zinc stearate[61]), 1398 and 1263 cm^{-1} (C—O/C—N stretching and in-ring deformations of antioxidant fragments[63]) and intensifies the band of 963 cm^{-1} belonging to SBR. The FTIR spectra show that DES modulates the chemical environment of the non-rubber components in NR, leading to limited changes in the sulfur bond distribution (Fig. S1 in ESI). The effects observed in the MB-DES systems may arise from their complementary roles in the Zn^{2+} accelerator curing system. MB contains heteroatom-bearing groups that are capable of weak coordination with Zn^{2+}, while DES provides a polar hydrogen-bond/ion-pair environment to modulate Zn^{2+} coordination. Therefore, their coexistence may interfere with the formation and stability of Zn^{2+}-containing intermediates, resulting in antioxidant-dependent variations in cure kinetics and crosslinking density. In the NR/SBR blends, DES modulates the vulcanization without influencing the S—S content.

Fig. 4 shows the TEM images of the vulcanizates filled with either 50 phr CB or 40 phr CB plus 10 phr BT. The composites with MB are shown as exemplars that demonstrate the effects of filler hybridization and DES addition. In all micrographs, the filler aggregates appear as dark areas. The introduction of DES and/or BT tends to improve filler dispersion by reducing agglomeration. This effect is more marked for DES. After thermo-oxidative aging, drastic morphological changes are not observed despite network degradation.

Mechanical Properties and Mullins Effect

According to the stress-strain (σ-ε) relationship curves (Fig. S2 in ESI), stresses at 100% and 300% strains and elongation at break are determined (Fig. S3 in ESI). For the virgin and aged vulcanizates, stresses at a given strain increase and elongation at break decreases with increasing v_c (Fig. S3 in ESI), which is related to the reduced extensibility of elastically effective strands in the densely crosslinked network.[64] In general, aging greatly lowers the strain at break and the tensile strength. The poor aging resistance of SBR vulcanizates involves marked post-vulcanization, which significantly increases v_c greatly. For NR and NR/SBR vulcanizates, the non-rubber components in NR[51] influence v_c and the redistribution of sulfur bonds[65,66] by promoting the generation of non-elastic network defects and additional crosslinks with a broader spatial distribution.[67,68] In composite vulcanizates, aging induces reductions in stress at 100% strain, elongation at break, and tensile strength, which is ascribed to network

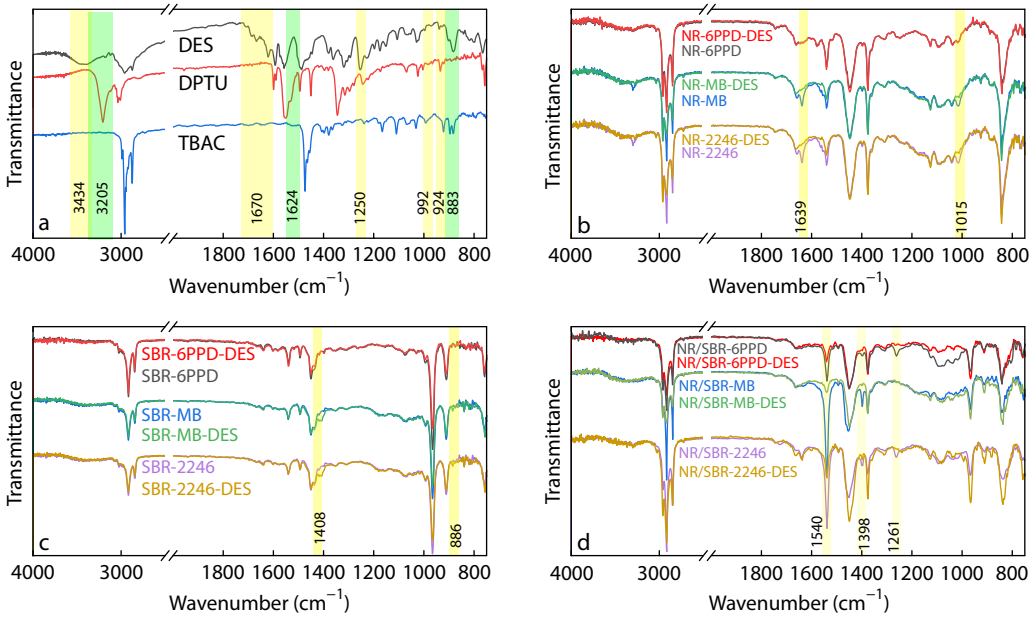

Fig. 3 FTIR spectra of (a) TBAC, DPTU, DES, (b) NR, (c) SBR, (d) NR/SBR vulcanizates. In (b–d), the thin curves represent the vulcanizates free of DES and the thick curves those containing DES.

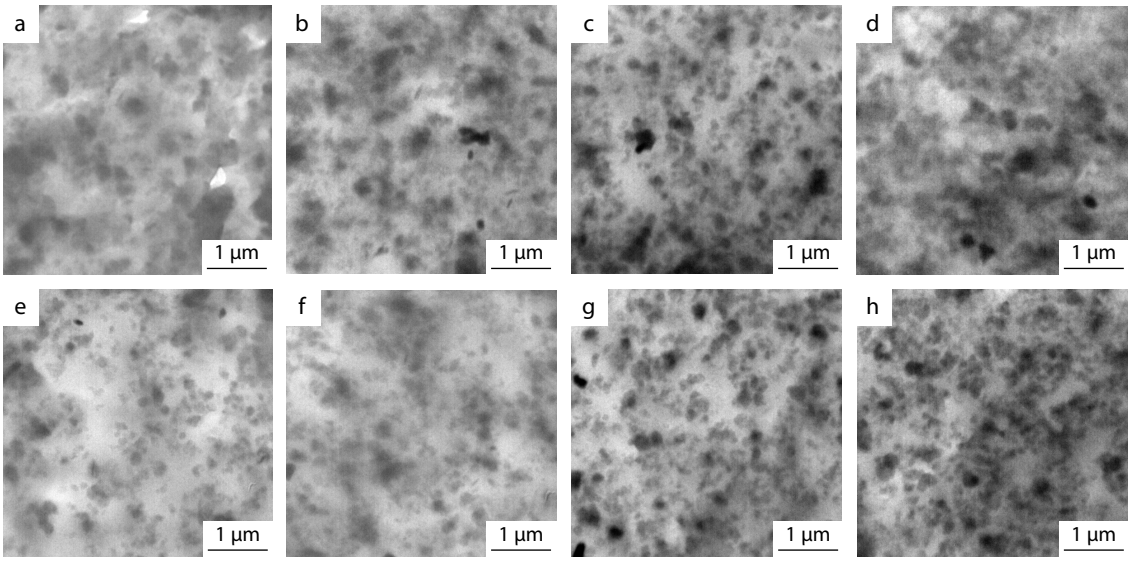

Fig. 4 TEM images of virgin (a–d) and aged (e–h) composites vulcanizates containing MB–CB/BT (a and e), MB-DES-CB/BT (b and f), MB-CB (c and g) and MB-DES-CB (d and h).

deterioration caused by chain scission, rearrangement of physical and chemical crosslinks, and filler–rubber interactions.[69]

The normalized stress $\sigma_n=\sigma/(\nu_c RT)$ is calculated for the virgin and aged vulcanizates (Fig. 5). Here, R is the gas constant and T is the absolute temperature. In SBR gum vulcanizates, DES rarely influences the mechanical properties, despite markedly improving the elongation at break in the absence of antioxidants. DES itself does not influence strain-induced crystallization (SIC) of NR vulcanizate free of antioxidants, while it promotes, delays, or does not influence SIC in the presence of 6PPD, MB, and 2246, respectively. In NR/SBR blend vulcanizates, DES promotes the SIC of NR and improves σ_n at high strains. This effect is more marked in those containing MB. In the composites, the σ_n curves of the virgin and aged vulcanizates at low strains approximately collapse, indicating the significant role of the filler that amplifies the microscopic deformation of the rubber phase.

The collapsed σ_n at low strains approximately follows the prediction of the Gaussian chain network model, $\sigma_n = \lambda - \frac{1}{\lambda^2}$, $\lambda = \varepsilon + 1$ being the drawn ratio. At high strains, the SIC of the NR causes substantial deviation in the NR and NR/SBR vulcanizates. For the non-crystallizable SBR vulcanizates, σ_n is approximated by tube theory[70] $\sigma_n = \left(\lambda - \frac{1}{\lambda^2}\right)\cdot\left\{\frac{1-T_e/n_e}{\left[1-T_e/n_e\left(\lambda^2+2/\lambda-3\right)\right]^2} - \frac{T_e/n_e}{1-T_e/n_e\left(\lambda^2+2/\lambda-3\right)}\right\} + \frac{2\nu_e}{\nu_c}\left(\frac{1}{\lambda^{1/2}} - \frac{1}{\lambda^2}\right)$ with entanglement density $\nu_e=4\nu_c$ and limiting extensibility $T_e/n_e=0$ for the low-extensible gum vulcanizates with antioxidants 6PPD, MB, and 2246, with $\nu_e=10\nu_c$ and $T_e/n_e=0.003$ for the highly extensible gum vulcanizates with DES. For composites in which the filler at volume fraction φ provides a strain amplification factor A_f,[71–73] the deformation at low strains could be approximated by a Gaussian chain network model incorporating the filler-induced strain amplification effect[53,71–73] $\sigma_n = A_f(1-\varphi)\left(\lambda_{mic} - \frac{1}{\lambda_{mic}^2}\right)$ with $\lambda_{mic} = A_f\varepsilon + 1$ and $A_f \approx 2.5$.

The vulcanizates experiencing cyclic stretching at 25 °C exhibit Mullins effect[74–79] being significantly enhanced by filling[71,80–82] (Figs. S4 and S5 in ESI). NR at strains above 5–6 undergoes SIC[83–85] that contributes to dissipation[86,87] by greatly lowering the percentage softening (E_s/E_h) and improving the percentage damping (E_h/E_3).[88–92] Here E_3 and E_h are the deformation and hysteresis energy densities in the third loading-unloading run, respectively, and E_s is the softening energy density estimated as the difference in hysteresis energy densities in the first and third runs. In comparison with NR, the SBR gum vulcanizates exhibit a weaker Mullins effect with percentage damping E_h/E_3=0.06, which is independent of prestrain (ε_{pre}) and antioxidants (Fig. S6 in ESI). The blending lowers E_h/E_3 and improves E_s/E_h at high ε_{pre}, which could be ascribed to the weakened contribution of the SIC of NR. In comparison with 6PPD, MB tends to elevate E_s of NR and lower E_s of SBR and blend vulcanizates. Fig. 6 shows the Mullins effect parameters, all increase with increasing ε_{pre}. Partial replacement of CB by BT causes reductions in E_s and E_s/E_h, which is significant in composites containing MB antioxidants. Such differences can be interpreted in terms of the network integrity and filler dispersion. Variations in ν_c affect the effective strand lengths, while the filler-network compactness influences the localized strain amplification and interfacial stress concentration. As suggested by the TEM images in Fig. 4, the comparatively more uniform and stable dispersion in the MB-DES-CB/BT system likely suppresses irreversible interfacial slippage during cyclic deformation, thereby lowering E_s. When CB is used as the filler, the introduction of DES does not influence the Mullins effect parameters. On the other hand, when CB and BT exist in the composites containing MB antioxidant, DES facilitates weakening the softening and greatly lowers E_s, which is beneficial for design and preparation of high strength (22.1 MPa, comparable with 23.4 MPa of the NR/SBR-CB composites) and low-dissipative rubber blend composites.

https://doi.org/10.1007/s10118-026-3632-7

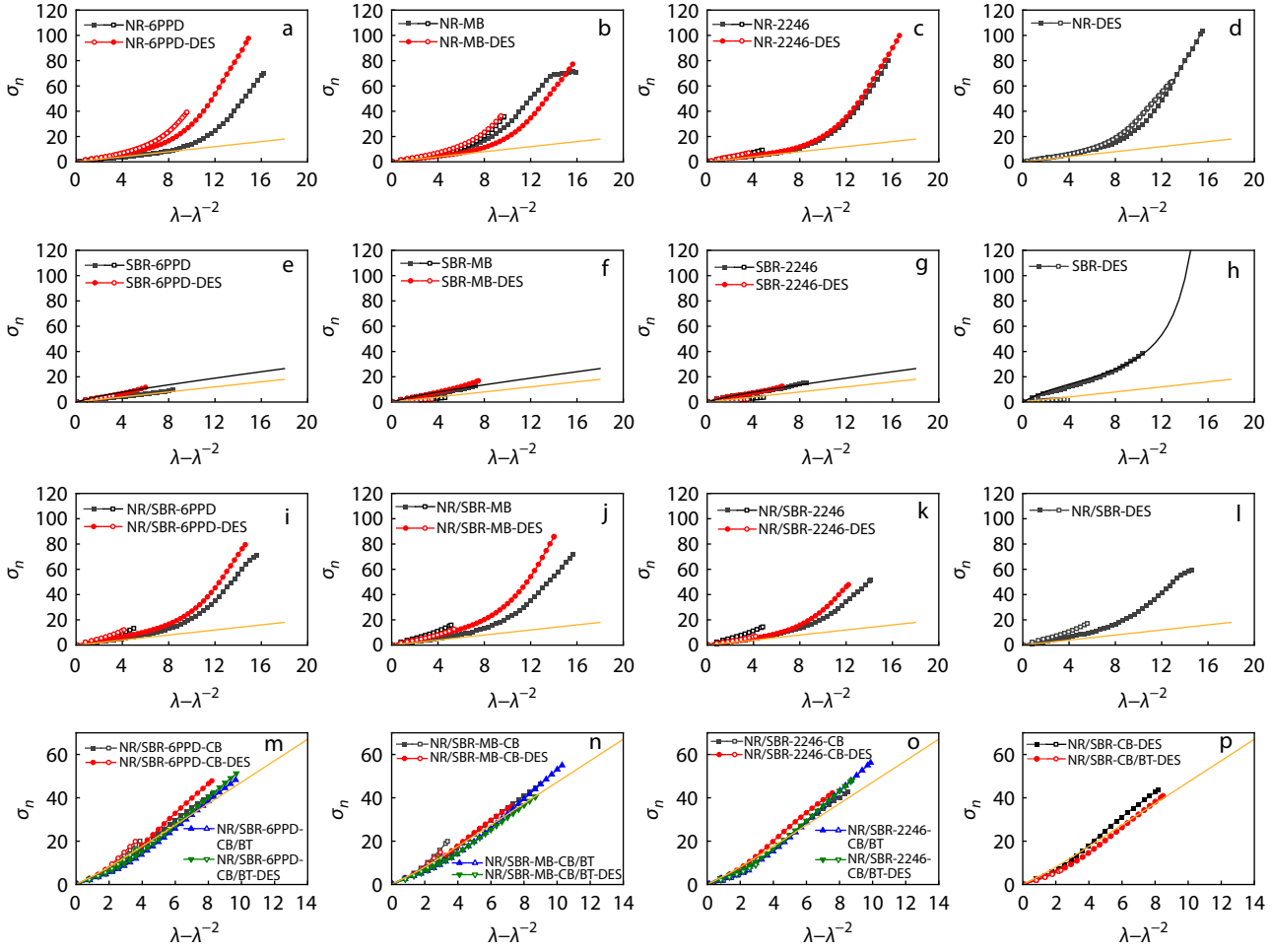

Fig. 5 Normalized stress σ_n against $\lambda - 1/\lambda^2$ at 25 °C for the virgin (solid symbols) and aged (hollow symbols) NR (a–d), SBR (e–h), NR/SBR (i–l), NR/SBR-CB and NR/SBR-CB/BT vulcanizates (m–p). The thick solid curves in (a–l) are drawn according to the prediction of Gaussian-chain network model, and those in (m–p) to the modified Gaussian-chain network model. In (e–h), thin curves are drawn according to the tube theory with $v_e = 4v_c$ and T_e/n_e=0 for the gum vulcanizates with antioxidants 6PPD, MB and 2246 and with $v_e = 10v_c$ and T_e/n_e=0.003 for those with DES.

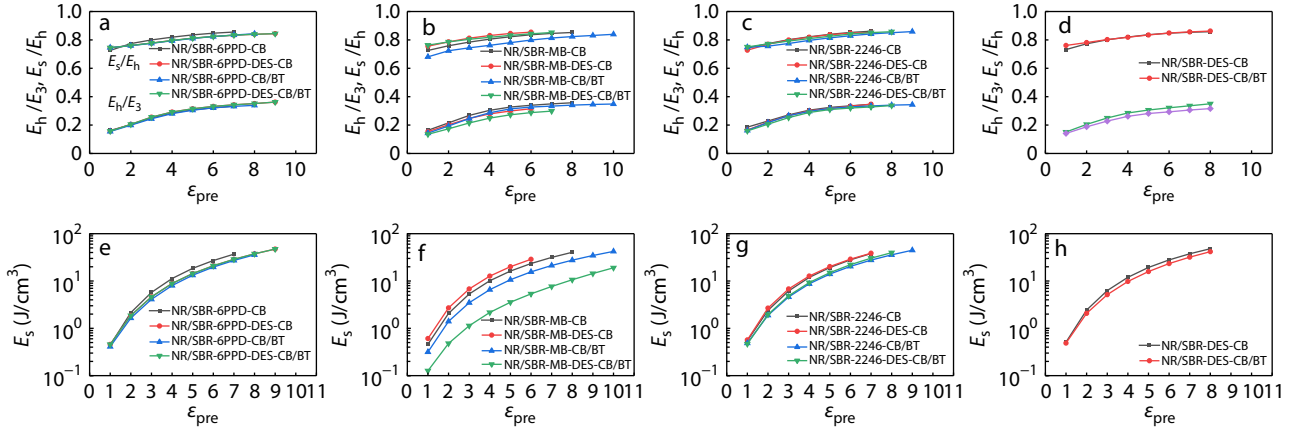

Fig. 6 Percentage softening (E_s/E_h, a–d), percentage damping (E_h/E_3, a–d), and softening energy density (E_s, e–h) as a function prestrain (ε_{pre}) for the NR/SBR-CB and NR/SBR-CB/BT composites vulcanizates containing 6PPD (a, and e), MB (b and f), 2246 (c and g) and DES (d and h).

CONCLUSIONS

DES markedly accelerates curing and shortens the induction period of the NR, SBR, and NR/SBR gums, and v_c of the vulcanizates is highly dependent on the antioxidants and DES. DES co-operates with the non-rubber constituents in NR so that the co-use of DES with MB facilitates the formation of a highly crosslinked network in the NR/SBR vulcanizates. A partial replacement of CB with BT weakens the Mullins softening, and the combination of MB with DES leads to the highest efficiency for

https://doi.org/10.1007/s10118-026-3632-7

weakening the Mullins effect. This work opens a fascinating window for preparing high-strength NR/SBR composite vulcanizates with a weakened Mullins effect. Given the structural tunability of DES, their integration with rubber blending, antioxidant selection, and filler hybridization offers a promising route to further regulate the strength, aging resistance, and Mullins behavior in high-performance rubber composites for scalable industrial applications.

Conflict of Interests

The authors declare no interest conflict.

Electronic Supplementary Information

Electronic supplementary information (ESI) is available free of charge in the online version of this article at http://doi.org/10.1007/s10118-026-3632-7.

Data Availability Statement

Data will be made available on request from the corresponding authors.

ACKNOWLEDGMENTS

This work was financially supported by the National Natural Science Foundation of China (No. 22533004).

REFERENCES

1 Kazemi, H.; Mighri, F.; Rodrigue, D. A review of rubber biocomposites reinforced with lignocellulosic fillers. *J. Compos. Sci.* **2022**, *6*, 183.
2 Alam, M. N.; Kumar, V.; Jung, H. S.; Park, S. S. Fabrication of high-performance natural rubber composites with enhanced filler-rubber interactions by stearic acid-modified diatomaceous earth and carbon nanotubes for mechanical and energy harvesting

Graphical Abstract

Influence of Antioxidants and Deep Eutectic Solvent on Vulcanization Kinetics and Mechanical Behaviors of Natural Rubber/Styrene-Butadiene Rubber Blend and Composites

Zi-Ye Liu, Yi-Hu Song, and Qiang Zheng

Zhejiang University

Deep eutectic solvent (DES) modulates vulcanization kinetics and crosslinking structure; when combined with MB and carbon black (CB)/black talc (BT), it facilitates the preparation of high-strength natural rubber (NR)/styrene-butadiene rubber (SBR) composites with reduced hysteresis and weakened Mullins effect.

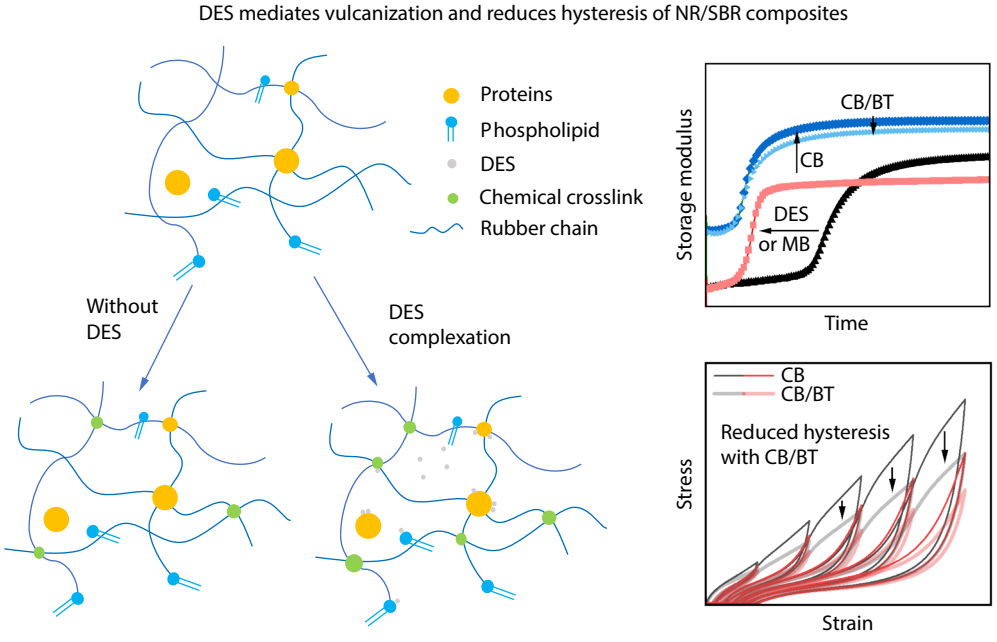

applications. *Polymers* **2023**, *15*, 3612.
3 Rajawasam, C. W. H.; Dodo, O. J.; Weerasinghe, M. A. S. N.; Raji, I. O.; Wanasinghe, S. V.; Konkolewicz, D.; Watuthanthrige, N. D. A. Educational series: characterizing crosslinked polymer networks *Polym. Chem*. **2024,** *15*, 219–247.
4 Sadequl, A. M.; Ishiaku, U. S.; Ismail, H.; Poh, B. T. The effect of accelerator/sulphur ratio on the scorch time of epoxidized natural rubber. *Eur. Polym. J.* **1998**, *34*, 51–57.
5 Poschl, M.; Sathi, S. G.; Stocek, R. Identifying the co-curing effect of an accelerated-sulfur/bismaleimide combination on natural rubber/halogenated rubber blends using a rubber process analyzer. *Polymers* **2021**, *13*, 4329.
6 Samarasinghe, I. H. K.; Walpalage, S.; Edirisinghe, D. G.; Egodage, S. M. Study on sulfur vulcanized natural rubber formulated with nitrosamine safe diisopropyl xanthogen polysulfide/tertiary butyl benzothiazole sulphenamide binary accelerator system. *Prog. Rubber Plast. Recycl. Technol.* **2020**, *37*, 190–202.
7 Charoeythornkhajhornchai, P.; Samthong, C.; Somwangthanaroj, A. Influence of sulfenamide accelerators on cure kinetics and properties of natural rubber foam. *J. Appl. Polym. Sci.* **2017**, *134*, 44822.
8 Gaca, M.; Vaulot, C. Effect of fillers modification with ils on fillers textural properties: thermal properties of SBR composites. *Int. J. Mole. Sci.* **2024**, *25*, 885.
9 Jung, W.; Cho, S.; Jang, K. Effect of surface-modified mica in hybrid filler systems on the curing and mechanical behavior of ethylene-propylene-diene monomer (EPDM)/butadiene rubber (BR) blend. *Polymers* **2025**, *17*, 2250.
10 Jovanovic, V.; Budinski Simendic, J.; Samardzija Jovanovic, S.; Markovic, G.; Marinovic Cincovic, M. The influence of carbon black on curing kinetics and thermal aging of acrylonitrile-butadiene rubber. *Chem. Ind. Chem. Eng. Q.* **2009**, *15*, 283–289.
11 Kruzelak, J.; Hlozekova, K.; Kvasnicakova, A.; Tomanova, K.; Hudec, I. Application of sulfur and peroxide curing systems for cross-linking of rubber composites filled with calcium lignosulfonate. *Polymers* **2022**, *14*, 1921.
12 Hosseini, S. M.; Razzaghi Kashani, M. Vulcanization kinetics of nano-silica filled styrene butadiene rubber. *Polymer* **2014**, *55*, 6426–6434.
13 Hosseini, S. M.; Razzaghi Kashani, M. On the role of nano-silica in the kinetics of peroxide vulcanization of ethylene propylene diene rubber. *Polymer* **2017**, *133*, 8–19.
14 Suresh, K.; Megavarnan, R.; Vengatachalam, P.; Krishnamurthy, S.; Balakrishnan, P. A review on the effect of various nano fillers on the mechanical properties and thermal stability of chloroprene rubber composites. *Mater. Today Proc.* **2022**, *68*, 2560–2568.
15 Liu, Y.; Li, L.; Wang, Q. Reinforcement of natural rubber with carbon black/nanoclay hybrid filler. *Plast Rubber Compos.* **2013**, *39*, 370–376.
16 Abdul Salim, Z. A. S.; Hassan, A.; Ismail, H. A review on hybrid fillers in rubber composites. *Polym. Plast. Technol. Eng.* **2017**, *57*, 523–539.
17 Poikelispää, M.; Shakun, A.; Sarlin, E. Nanodiamond—carbon black hybrid filler system for demanding applications of natural rubber—butadiene rubber composite. *Appl. Sci.* **2021**, *11*, 10085.
18 Zou, M.; Gao, W.; Li, Z.; Liu, B.; Li, B.; Liu, K.; Liu, J. Hybrid carbon black/silica reinforcing system for high-performance green tread rubber. *Polymers* **2024**, *16*, 2762.
19 Vayyaprontavida Kaliyathan, A.; Varghese, K. M.; Nair, A. S.; Thomas, S. Rubber–rubber blends: a critical review. *Prog. Rubber Plast. Recycl. Technol.* **2019**, *36*, 196–242.
20 Li, C.; Song, Y. Effects of ionic liquid on strain softening behaviors of silica filled natural rubber/nitrile butadiene rubber nanocomposites. *Acta Polymerica Sinica* (in Chinese) **2024**, *55*, 1549–1560.
21 Tang, S.; Li, Z.; Sun, W.; Liu, Y.; Wang, J.; Wang, X.; Lin, J. Natural rubber/styrene-butadiene rubber blend composites potentially applied in damping bearings. *Polymers* **2024**, *16*, 1945.
22 Findik, F.; Yilmaz, R.; Köksal, T. Investigation of mechanical and physical properties of several industrial rubbers. *Mater. Des.* **2004**, *25*, 269–276.
23 Chen, Q.; Huang, W.; Zhang, L.; Chen, Y.; Liu, J. Impact of sacrificial hydrogen bonds on the structure and properties of rubber materials: insights from all-atom molecular dynamics simulations. *Langmuir* **2024**, *40*, 11470–11480.
24 Hu, R.; Zhao, S.; Chen, F.; Shangguan, Y.; Zheng, Q. Effect of sacrificial bond on molecular dynamics and rheological behavior of hybrid butadiene-styrene-vinylpyridine rubber vulcanizates with reversible sacrificial network. *J. Polym Sci*. **2022**, *60*, E1–E12.
25 Imbernon, L.; Norvez, S. From landfilling to vitrimer chemistry in rubber life cycle. *Eur. Polym. J.* **2016**, *82*, 347–376.
26 Denissen, W.; Winne, J. M.; Du Prez, F. E. Vitrimers: permanent organic networks with glass-like fluidity. *Chem Sci* **2016**, *7*, 30–38.
27 Langley, N. R. Elastically effective strand density in polymer networks. *Macromolecules* **2002**, *1*, 348–352.
28 Han, Q.; Li, X.; Li, Y.; Wu, Y. Influences of the compatibility of NR/SSBR and phase-selective distribution of silica on its static and dynamic properties. *Rubber Chem. Technol.* **2020**, *93*, 588–604.
29 Le, H. H.; Hamann, E.; Ilisch, S.; Heinrich, G.; Radusch, H. J. Selective wetting and dispersion of filler in rubber composites under influence of processing and curing additives. *Polymer* **2014**, *55*, 1560–1569.
30 Aswathy, T. R.; Dash, B.; Dey, P.; Nair, S.; Naskar, K. Synergistic effect of graphene with graphene oxide, nanoclay, and nanosilica in enhancing the mechanical and barrier properties of bromobutyl rubber/epoxidized natural rubber composites. *J. Appl. Polym. Sci.* **2021**, *138*, 50746.
31 Azizli, M. J.; Barghamadi, M.; Rezaeeparto, K.; Mokhtary, M.; Parham, S. Compatibility, mechanical and rheological properties of hybrid rubber NR/EPDM-*g*-MA/EPDM/graphene oxide nanocomposites: theoretical and experimental analyses. *Compos. Commun.* **2020**, *22*, 100442.
32 Zhao, X.; Niu, K.; Xu, Y.; Peng, Z.; Jia, L.; Hui, D.; Zhang, L. Morphology and performance of NR/NBR/ENR ternary rubber composites. *Compos, B* **2016**, *107*, 106–112.
33 Phiriyawirut, M.; Luamlam, S. Influence of poly(vinyl chloride) on natural rubber/chlorosulfonated polyethylene blends. *Open J. Org. Polym. Mater.* **2013**, *03*, 81–86.
34 Zhao, H.; Xiang, Y.; Wu, L.; Gao, J. Effect of compatibilizer on properties of chloroprene rubber/natural rubber blends. *Polym. Bull.* **2022**, *35*, 65–71.
35 Karekar, A.; Oßwald, K.; Reincke, K.; Langer, B.; Saalwächter, K. NMR studies on the phase-resolved evolution of cross-link densities in thermo-oxidatively aged elastomer blends. *Macromolecules* **2020**, *53*, 11166–11177.
36 Sidkey, M. A.; Yehia, A. A.; Abd El Malak, N. A.; Gaafar, M. S. Compatibility studies on some rubber blend systems by ultrasonic techniques. *Mater. Chem. Phys.* **2002**, *74*, 23–32.
37 Stabile, P.; Mastinu, G.; Gobbi, M.; Bardini, P. Tire aging: a state-of-the-art review. *Eng. Sci. Technol. Int. J.* **2025**, *69*, 102101.
38 Bensalem, K.; Eesaee, M.; Hassanipour, M.; Elkoun, S.; David, E.; Agbossou, K.; Nguyen-Tri, P. Lifetime estimation models and degradation mechanisms of elastomeric materials: a critical review. *Polym. Degrad. Stabil.* **2024**, *220*, 110644.
39 Taourit, S.; Gac, P. Y. L.; Bourdet, A.; Van Elslander, A.; Robin, C.; Fayolle, B. Changes in natural rubber mechanical behavior during oxidation: relationship with oxygen consumption. *Polym. Degrad. Stabil.* **2024**, *225*, 110787.

https://doi.org/10.1007/s10118-026-3632-7

40 Xuan, Y. Y.; Ridzuan, M. J. M.; Majid, M. S. A.; Marsi, N.; Rahman, M. T. A.; Yudhanto, F.; Sapuan, S. M. Effect of thermal aging on the tensile and tribological properties of pineapple leaf fiber-reinforced natural rubber composites incorporating multiwalled carbon nanotubes. *Polym. Compos.* **2025**, *46*, 15637–15651.

41 Ferradino, A. G. Antioxidant selection for peroxide cure elastomer applications. *Rubber Chem. Technol.* **2003**, *76*, 694–718.

42 Xu, J.; Hao, Y.; Yang, Z.; Li, W.; Xie, W.; Huang, Y.; Wang, D.; He, Y.; Liang, Y.; Matsiko, J.; Wang, P. Rubber antioxidants and their transformation products: environmental occurrence and potential impact. *Int. J. Environ. Res. Public Health* **2022**, *19*, 14595.

43 Zidan, T. A.; Kandil, H. S. Investigation of novel polyanilines as new antioxidants for ethylene propylene diene monomer rubber composites. *J. Appl. Polym. Sci.* **2023**, *141*, 54924.

44 Liu, F.; Liu, Z.; Hou, G.; Lin, G.; Tian, Z.; Zhao, M.; Huang, Z.; Zhang, Y. Improving dispersion of alkali lignin in natural rubber by adopting graphene oxide as a carrier. *ACS Appl. Polym. Mater.* **2024**, *6*, 10927–10935.

45 Xie, X.; Wu, L.; He, J.; Liu, F. Preparation of chitosan-based macromolecular antioxidant with high-efficiency free radical scavenging ability to improve the antioxidative properties of styrene-butadiene rubber/silica composites. *Compos. Commun.* **2024**, *51*, 102098.

46 Zhao, W.; He, J.; Yu, P.; Jiang, X.; Zhang, L. Recent progress in the rubber antioxidants: a review. *Polym. Degrad. Stabil.* **2023**, *207*, 110223.

47 Yang, L.; Sun, S.; Yu, X.; Xu, Z.; Lu, Y.; Shi, X.; Song, Y.; Wang, D.; Zuo, M.; Zheng, Q. Effect of deep eutectic solvents on vulcanization kinetics and strain-softening behavior of natural rubber/styrene-butadiene rubber. *Polymer* **2025**, *316*, 127871.

48 Li, Q.; Liu, B.; Hu, Z.; Jiang, X.; Yang, L.; Meng, H.; Song, Y.; Zheng, Q. Preparation of deep eutectic solvents based on metal ions and their influences on reinforcement and strain softening behaviors of silica filled natural rubber nanocomposites. *Compos, A* **2024**, *181*, 108119.

49 Flory, P. J.; Rehner, J. Statistical mechanics of cross-linked polymer networks. II. Swelling. *J. Chem. Phys.* **1943**, *11*, 521–526.

50 Dzulkifli, A. I.; Said, C. M. S.; Han, C. C.; Mohd, A. F. Rubber-solvent interaction parameter ($\chi_{1,2}$) of NR/SBR rubber blend solution in determination of crosslink concentration for vulcanized rubber blend. *Adv. Mater. Res.* **2015**, *1134*, 75–81.

51 Guo, Y.; Han, D.; Tian, X.; Ma, D.; Wu, X.; Han, D.; Yang, N.; Zhang, J. Quantitative determination of non-rubber components and construction of supramolecular network aggregation state structure of natural rubber. *Ind. Crops Prod.* **2025**, *227*, 120846–120855.

52 Sotta, P.; Albouy, P. A.; Abou Taha, M.; Moreaux, B.; Fayolle, C. Crosslinked elastomers: structure-property relationships and stress-optical law. *Polymers* **2021**, *14*, 9.

53 Shen, J.; Lin, X.; Liu, J.; Li, X. Effects of cross-link density and distribution on static and dynamic properties of chemically cross-linked polymers. *Macromolecules* **2018**, *52*, 121–134.

54 Liu, C.; He, J.; Ruymbeke, E. V.; Keunings, R.; Bailly, C. Evaluation of different methods for the determination of the plateau modulus and the entanglement molecular weight. *Polymer* **2006**, *47*, 4461–4479.

55 Wu, K.; Wang, X. Transition of rheological responses to linear-nonlinear dichotomy: the role of polymers in particle-filled solutions. *Macromolecules* **2024**, *57*, 6593–6605.

56 Litvinov, V. M.; Orza, R. A.; Klüppel, M.; van Duin, M.; Magusin, P. C. M. M. Rubber–filler interactions and network structure in relation to stress–strain behavior of vulcanized, carbon black filled epdm. *Macromolecules* **2011**, *44*, 4887–4900.

57 Robertson, C. G.; Hardman, N. J. Nature of carbon black reinforcement of rubber: perspective on the original polymer nanocomposite. *Polymers* **2021**, *13*, 538.

58 Wei, Y.; Xie, W.; He, M.; Zhu, D.; Liu, S.; Zhang, L.; Liao, S. The role of non-rubber components acting as endogenous antioxidants on thermal-oxidative aging behavior of natural rubber. *Polym. Test.* **2022**, *111*, 107614.

59 Yang, W.; Zhou, W.; Zhang, Z. Structural and spectroscopic study on *N*-2-fluorobenzoyl-*N*′-4-methoxyphenylthiourea. *J. Mole. Struct.* **2007**, *828*, 46–53.

60 Rolere, S.; Liengprayoon, S.; Vaysse, L.; Sainte-Beuve, J.; Bonfils, F. Investigating natural rubber composition with fourier transform infrared (FT-IR) spectroscopy: a rapid and non-destructive method to determine both protein and lipid contents simultaneously. *Polym. Test.* **2015**, *43*, 83–93.

61 Ikeda, Y.; Sakaki, Y.; Yasuda, Y.; Junkong, P.; Ohashi, T.; Miyaji, K.; Kobayashi, H. Roles of dinuclear bridging bidentate zinc/stearate complexes in sulfur cross-linking of isoprene rubber. *Organometallics* **2019**, *38*, 2363–2380.

62 ŠKulteckĖ, J.; BitarytĖ, S.; Liubinas, K. FTIR-ATR spectroscopy to identify and quantify the SBS in modified bitumen. In *12th International Conference Environmental Engineering*, Vilnius, Lithuania, **2023**, p. 1–6.

63 Smith, B. C. The infrared spectra of polymers. VI: Polymers with C-O bonds. *Spectroscopy* **2022**, *37*, 15–19, 27.

64 Hayeemasae, N.; Waesateh, K.; Soontaranon, S.; Masa, A. Effect of vulcanization systems and crosslink density on tensile properties and network structures of natural rubber. *J. Technol.* **2022**, *84*, 181–187.

65 Wei, Y.; Liu, G.; Zhang, L.; Zhao, F.; Liao, S.; Luo, M. Exploring the unique characteristics of natural rubber induced by coordination interaction between proteins and Zn^{2+}. *Polymer* **2020**, *193*, 122357–122362.

66 Wang, M.; Wang, R.; Chen, X.; Kong, Y.; Huang, Y.; Lv, Y.; Li, G. Effect of non-rubber components on the crosslinking structure and thermo-oxidative degradation of natural rubber. *Polym. Degrad. Stabil.* **2022**, *196*, 109845–109855.

67 Nimpaiboon, A.; González-Jiménez, A.; Pérez-Aparicio, R.; Martín-Salamanca, F.; Zepeda-Rodríguez, Z.; López-Valentín, J.; Sakdapipanich, J. Effect of proteins on the network formation and degradation of peroxide cross-linked natural rubber elucidated by time-domain NMR. *Polymers* **2025**, *17*, 1063–1086.

68 He, C. Z.; Peng, Z.; Zhong, J. P.; Liao, S. Q.; She, X. D.; Luo, Y. Y.; Tan, H. S. Thermal and thermo-oxidative degradations of deproteinized natural rubber and natural rubber. *Adv. Mater. Res.* **2011**, *306–307*, 50–57.

69 Omnès, B.; Thuillier, S.; Pilvin, P.; Grohens, Y.; Gillet, S. Effective properties of carbon black filled natural rubber: Experiments and modeling. *Compos, A* **2008**, *39*, 1141–1149.

70 Klüppel, M.; Schramm, J. A generalized tube model of rubber elasticity and stress softening of filler reinforced elastomer systems. *Macromol. Theory Simul.* **2000**, *9*, 742–754.

71 Song, Y.; Zheng, Q. Concepts and conflicts in nanoparticles reinforcement to polymers beyond hydrodynamics. *Prog. Mater Sci.* **2016**, *84*, 1–58.

72 Song, Y.; Zheng, Q. A guide for hydrodynamic reinforcement effect in nanoparticle-filled polymers. *Crit. Rev. Solid State Mater. Sci.* **2016**, *14*, 318–346.

73 Song, Y.; Wu, G.; Wang, D.; Peng, J.; Zhang, C.; Zheng, Q. Tailoring reinforcement and strain softening behaviors of natural rubber vulcanizates nanocomposites by dopamine-modified silica. *Compos. B* **2023**, *254*, 110552.

74 Roland, C. M. The mullins effect in crosslinked rubber. *J. Rheol.* **1989**, *33*, 659–670.

75 Diani, J.; Fayolle, B.; Gilormini, P. A review on the Mullins effect.

Eur. Polym. J. **2009**, *45*, 601–612.
76 Harwood, J. A. C.; Mullins, L.; Payne, A. R. Stress softening in natural rubber vulcanizates. Part II. Stress softening effects in pure gum and filler loaded rubbers. *J. Appl. Polym. Sci.* **1965**, *9*, 814–822.
77 Harwood, J. A. C.; Payne, A. R. Stress softening in natural rubber vulcanizates. Part IV. Unfilled vulcanizates. *J. Appl. Polym. Sci.* **1966**, *10*, 1203–1211.
78 Han, J.; Wei, C.; Lu, A.; Song, K.; Zhang, Q.; Sun, G.; Xu, J.; Li, Z.; Liu, D. Visualizing filler network to reveal structural mechanisms on energy dissipation of mullins effect in silicone rubber. *Polymer* **2024**, *301*, 1–7.
79 Kittur, M. I.; Andriyana, A.; Ang, B. C.; Ch'ng, S. Y.; Verron, E. Inelastic response of thermo-oxidatively aged carbon black filled polychloroprene rubber. Part II: Mullins effect. *Polym. Degrad. Stabil.* **2022**, *204*, 110120.
80 Watson, W. F. Combination of rubber and carbon black on cold milling. *Ind. Eng. Chem.* **1955**, *47*, 1281–1286.
81 Leblanc, J. L. Rubber-filler interactions and rheological properties in filled compounds. *Prog. Polym. Sci.* **2002**, *27*, 627–687.
82 Kida, N.; Ito, M.; Yatsuyanagi, F.; Kaido, H. Studies on the structure and formation mechanism of carbon gel in the carbon black filled polyisoprene rubber composite. *J. Appl. Polym. Sci.* **1996**, *61*, 1345–1350.
83 Candau, N.; Chazeau, L.; Chenal, J.-M.; Gauthier, C.; Munch, E. Compared abilities of filled and unfilled natural rubbers to crystallize in a large strain rate domain. *Compos. Sci. Technol.* **2015**, *108*, 9–15.
84 Trabelsi, S.; Albouy, P. A.; Rault, J. Effective local deformation in stretched filled rubber. *Macromolecules* **2003**, *36*, 9093–9099.
85 Chen, L.; Wu, L.; Song, L.; Xia, Z.; Lin, Y.; Chen, W.; Li, L. The recovery of nano-sized carbon black filler structure and its contribution to stress recovery in rubber nanocomposites. *Nanoscale* **2020**, *12*, 24527–24542.
86 Trabelsi, S.; Albouy, P. A.; Rault, J. Crystallization and melting processes in vulcanized stretched natural rubber. *Macromolecules* **2003**, *36*, 7624–7639.
87 Le Cam, J. B. Energy storage due to strain-induced crystallization in natural rubber: the physical origin of the mechanical hysteresis. *Polymer* **2017**, *127*, 166–173.
88 Hou, F.; Song, Y.; Zheng, Q. Influence of liquid isoprene rubber on strain softening of carbon black filled isoprene rubber nanocomposites. *Chinese J. Polym. Sci.* **2021**, *39*, 887–895.
89 Hou, F.; Xia, Z.; Song, Y.; Chen, W.; Zheng, Q. Strain softening of bimodal isoprene rubber vulcanizates. *Macromol. Mater. Eng.* **2021**, *306*, 2000802.
90 Li, Z.; Wen, F.; Hussain, M.; Song, Y.; Zheng, Q. Scaling laws of mullins effect in nitrile butadiene rubber nanocomposites. *Polymer* **2020**, *193*, 122350.
91 Li, Z.; Xu, H.; Xia, X.; Song, Y.; Zheng, Q. Energy dissipation accompanying mullins effect of nitrile butadiene rubber/carbon black nanocomposites. *Polymer* **2019**, *171*, 106–114.
92 Qi, X.; Wang, L.; Zhang, Y.; Jia, M.; Zhang, L.; Yue, D. Second natural rubber with self-reinforcing effect based on strain-induced crystallization. *Macromolecules* **2022**, *55*, 2758–2767.

https://doi.org/10.1007/s10118-026-3632-7